Inversion of He-Ne elastic-scattering data

D. R. Lun, Xue Jun Chen,* L. J. Allen and K. Amos
School of Physics, University of Melbourne, Parkville, Victoria 3052, Australia
(Received 10 March 1994)

Quantal and semiclassical (WKB) methods of inversion have been used in an analysis of the elastic-scattering cross sections for 62.5-meV He atoms from Ne atoms by which an effective local interaction between those atoms is specified. The potentials obtained by the approximate method (WKB) differ from that found with the full quantal analysis. The quantal inversion potential is repulsive at short distances and becomes attractive at a radius of 2.695 Å. It has a minimum value of −1.981 meV at a radius of 2.98 Å.

PACS number(s): 34.40.+n

I. INTRODUCTION

Experimental and theoretical studies of interatomic and intermolecular potentials are important for a wide range of studies in chemistry, physics, and material science. Of the experimental set, those using molecular beams [1] are useful by giving data that directly reflect the detailed properties of intermolecular potentials, with those cases that do not form compounds under ordinary conditions being particularly interesting [2]. In the last decade, scattering experiments of atomic ions, neutral atoms, and molecules from atomic and molecular targets have been made with considerable precision and the definition of interatomic potentials from those data are of current interest [3].

Our interest is taken with the results of recent high resolution measurements of the differential cross sections from the elastic scattering of He atoms from Ne atoms [4]. That data are of high quality and their analysis may facilitate an accurate specification of the interatomic potential. In making such analyses, there are two distinctively different approaches one can consider. They are the "direct" methods of analysis and the "inversion" ones. Direct methods of analysis of (elastic-) scattering data involve repeated solution of the radial Schrödinger equations with an input central, local interaction that one believes appropriate to describe the (He-Ne) interaction. Usually that potential is chosen to be of some specific form, which is defined by a set of (relatively few) open parameters. The values of those parameters are adjusted and the cross sections predicted (from the phase shifts obtained by solving the radial Schrödinger equations) until prediction fits the observed data as well as possible. That "best fit" may be defined by a minimal value of the χ^2 of the fit to the measured data. A better measure from a statistical viewpoint, however, is the value of χ^2 per degree of freedom, (χ^2/F), wherein the definition of the degrees of freedom is the number of data points in the fitting process minus the number of free parameters used to make that fit. The direct procedure allows one to keep the numbers of free parameters small and also to choose a form that is realistic, i.e., the potential has a shape consistent with what other data and/or microscopic calculations of that interaction suggest. However, one is then limited to this *a priori* chosen form so that the minimization search is very constrained and, usually, the resultant (χ^2) or (χ^2/F) are large; the latter being much larger than a statistically good value, ca. 1.

Alternatively, one can treat the problem as one of fixed energy inverse scattering. In that approach there are diverse methods by which an effective, local potential can be extracted from the scattering data [5]. As with the direct methods, in inverse scattering theories, the S function plays an intermediary role. The inverse scattering methods of interest find the mappings of S functions to potentials. However, there is ambiguity in extracting the S function from the differential cross section data. Furthermore, cross section predictions only correlate with the values of the S functions at real integer values of the angular momentum. The inversion procedures require that the S function be defined for all complex values of the angular momentum. Thus there is an interpolation and extrapolation involved in this step of the analysis. Nevertheless, by choosing a specific class of S functions, and one for which stable and accurate solutions of the inverse scattering equations can be found, a potential can be specified that is free, essentially, of *a priori* assumptions about its shape, and whose use in a direct solution of the Schrödinger equation reproduces the S function with which one started and, concomitantly, the same quality of fit to the measured data. Naturally the potential will belong to that class of potentials associated with the chosen S function form. But the crucial factor is that one controls the quality of the fit to the cross section data. The inversion potentials we seek, ultimately, are ones for which the χ^2/F fits are of order unity.

Inverse scattering analyses of atomic scattering data have been made in the past and an excellent review of those has been written by Buck [6]. However, most have used semiclassical schemes to facilitate studies. Herein,

*Permanent address: Physics Department, Tsinghua University, Beijing, The Peoples Republic of China.

we have used a semiclassical (WKB) method of analysis as well but also we have solved the fully quantum mechanical problem. The S functions used in both calculations are essentially the same so that comparison of the two results (for a given energy) reflects the accuracy of the (easier to use) semiclassical method of analysis. Specifically, we study the cross section from the elastic scattering of 62.5 meV He atoms from Ne atoms. The measured data must be deconvoluted since they encompass a range of input velocities and an extended scattering volume. We use the deconvolution method as proposed by Shapiro and Gerber [7] with a slight modification. That deconvolution is considered briefly in the next section for completeness. Likewise, the inversion methods are given subsequently (Sec. III) before the results we have obtained are presented and discussed (Sec. IV).

II. THE DECONVOLUTION PROCEDURE

The experimental differential cross section [4] has well-resolved oscillations but, given the experimental arrangement, it is a convolution over scattering angles and projectile velocities. Those averaging effects introduce considerable distortions upon the monochromatic, angle resolved cross section that is required in the inversion process. Thus the relevant cross section must be extracted from the data by deconvolution. To do this, we have chosen the method proposed by Shapiro and Gerber [7] but with a slight modification to their chosen procedure.

This deconvolution begins with the relationship between the averaged cross sections in the laboratory system, $\sigma^L_{\rm av}$, and the idealized ones in the center of mass system, $\sigma^{\rm C}$, namely

$$\sigma^L_{\rm av}(\theta_L) = \int\int F(\theta_L,\theta,v)\ \sigma^{\rm C}(v,\theta)\ d\theta dv. \tag{1}$$

In general, the folding factor F, is very complicated. However, within the large limits of up to 10% full width at half maximum (FWHM) of the magnitude and 5° angular divergence for the primary beam and of up to 20% FWHM and 10° angular divergence for the secondary beam [7], which is the case in this experiment, F can be simplified as a separable form, so that

$$\begin{aligned}\sigma^{\rm C_{av}}(v_g,\theta) &= J\sigma^L_{\rm av} \\ &= \int_{v=0}^{\infty}\int_{\theta'=0}^{\pi} F_v(v_g - v)\ F_A(\theta-\theta') \\ &\quad \times\sigma^{\rm C}(v,\theta')\ dvd\theta' ,\end{aligned} \tag{2}$$

where J is the Jacobian for the transformation from the laboratory to the center of mass system and v_g is the centroid of the velocity distribution function. Both distribution functions can be approximated well by the simple forms

$$F_v(v_g - v) = D_v \exp[-B_v(v - v_g)^2] \tag{3}$$

and

$$F_A(\theta-\theta') = \begin{cases} D_A, & \theta-\delta \le \theta' \le \theta+\delta\ , \\ 0 & \text{otherwise}\ , \end{cases} \tag{4}$$

although the angular resolution may depend on the deflection angle. Indeed, for the experimental data of interest herein [4],

$$\delta = 0.8(1 + 0.044\theta)\ . \tag{5}$$

To effect the integrations, the cross section in the integrand is approximated by a sum of Gaussian peaks, viz.

$$\sigma^{\rm C}(v,\theta) = \sum_i v^\beta A_i \exp[-B_i(v\theta^{1/\alpha} - \bar{v}\theta_i^{1/\alpha})^2]\ , \tag{6}$$

wherein $\bar{v}$ is the average velocity (essentially v_g) and the scaling powers are taken as 0.95 and 1.25 for α and β, respectively. The coefficients, A_i, B_i and θ_i, are adjusted to provide the best fit. With this form, one finds

$$\sigma^{\rm C}_{\rm av}(v_g,\theta) = \sum_i \xi_i(v_g)\int_0^\pi F_A(\theta-\theta')P_i(\theta')d\theta'\ , \tag{7}$$

where

$$\xi_i(v_g) = v_g^\beta A_i D_v\ , \tag{8}$$

and

$$\begin{aligned}P_i(v_g,\theta) &= \sqrt{\frac{\pi}{B_v + B_i\theta^{2/\alpha}}} \\ &\quad \times \exp\left[-\frac{B_vB_i(v_g\theta^{1/\alpha} - \bar{v}\theta_i^{1/\alpha})^2}{B_v + B_i\theta^{2/\alpha}}\right]\ .\end{aligned} \tag{9}$$

The final integration over v is facilitated by a further simple approximation [7]; the attendant error being negligible.

Shapiro and Gerber [7] used a fitting-iterative deconvolution procedure to ascertain a relevant parameter set. Instead, we have found those parameters, A_i, B_i, and θ_i, directly by a χ^2 minimization; i.e., by minimization of

$$\chi^2 = \sum_n \left[\frac{\sigma_{\rm av}(\theta_n) - \sum \xi_i(v_g)\ \int_0^\pi F_A(\theta_i-\theta')\ P_i(\theta')\ d\theta'}{\Delta\sigma_n}\right]^2 \tag{10}$$

Using our procedure, an excellent fit to the measured data for 62.5 meV He atoms from Ne atoms gave the set of Gaussian parameters we present in Table I. With ten Gaussian peaks in the fitting process, the best fit had a value of 58 for the χ^2 defined above. Therewith, the deconvoluted cross section can be specified for all scattering angles. But, in the inversion analyses, we will use that cross section only at the angles specified by the experiment and associate with that set of values the uncertainties as given by the experiment as well.

TABLE I. The parameters of the Gaussian forms used in deconvoluting the cross sections. The numbers in brackets denote multiplicative powers of ten.

A_i	B_i	θ_i
1.06708[2]	5.66234[−1]	6.04782
−4.39140	8.20492[−1]	9.11027
2.99443[1]	2.13439[−1]	1.16856[1]
9.68774	1.97581[−1]	1.83995[1]
3.19770	9.24141[−2]	2.49362[1]
2.41473	1.19061[−3]	2.95319[1]
1.13769	1.39315[−1]	3.19565[1]
1.27947[−1]	1.02282[−1]	3.91891[1]
5.9232[−1]	1.25424[−3]	6.14500[1]
1.11797	1.79943[−4]	9.59434[1]

III. THE INVERSION METHODS

In the following, we discuss two inversion procedures suitable for use in analyses of atom-atom elastic-scattering data.

A. Quantal inversion

Fully quantal inversion schemes of the Lipperheide–Fiedeldey type have been used successfully also to analyze the elastic-scattering cross sections from nucleus-nucleus [8,9], electron-atom [10], and electron-molecule [11] scattering.

In the simplest of those schemes, one assumes the total S function to be of the rational form given by

$$S_{\rm rat}(\lambda) = \frac{\prod_{n=1}^{N}(\lambda^2-\beta_n^2)}{\prod_{m=1}^{N}(\lambda^2-\alpha_m^2)} , \tag{11}$$

as the potential associated with such an S function is given by

$$V(r) = V_N(r) , \tag{12}$$

namely, the $N^{\rm th}$ iterate of

$$V_n(r) = V_{n-1}(r) + V^{(n)}(r) \quad , \quad n = 1,\ldots,N , \tag{13}$$

when, with the $n^{\rm th}$ pole-zero pair, $\{\alpha_n,\beta_n\}$,

$$V^{(n)}(r) = \frac{2}{r}(\beta_n^2-\alpha_n^2)\frac{d}{dr}\left[\frac{1}{r}\frac{1}{L_{\beta_n}^{(n-1)}(r)-L_{\alpha_n}^{(n-1)}(r)}\right] . \tag{14}$$

Therein, $L_\lambda^{(\pm)}(r)$ are the logarithmic derivatives of the Jost solutions $f_\lambda^{(\pm)}(r)$ to the potential $V_{n-1}(r)$ that asymptote as $e^{\mp ikr}$ respectively. Thus the potential is determined entirely by the poles and zeros of the S function. While in general the potential is complex, it will be real if α_n and β_n are complex conjugates for all n. This is a constraint which we have applied in the studies to be discussed.

One can also include a given background potential V_0 provided solutions can be found for the underlying Ricatti-Bessel equations that specify all iterates of the ensuing series to define $V_N(r)$. The advantage of using a background interaction in this scheme is to keep the number of pole-zero pairs to a minimum and of sizes that do not cause numerical difficulties with the inversion. Then the set of pole-zero pair values of the rational S function required are those that relate to use of a product form

$$S(\lambda) = S_{\rm ref}(\lambda)S_{\rm rat} . \tag{15}$$

We have used a reference S function, $S_{\rm ref}$, associated with a potential having the form $A\exp(-Br)$. The deconvoluted cross section for the 62.5 meV He-Ne scattering can be well fitted with such an S function form and with but a set of three pole-zero pair values. Specifically, with the exponential reference potential parameter values, A and B, of 797 eV and 4.03 Å^{-1}, respectively, the deconvoluted cross section was fitted well with the set of complex conjugate pole-zero pair values as listed in Table II. The significant factors for numerical stability and to have monotonic variation in $V(r)$ for large radii, are the relatively large values > 1.5 of the imaginary parts. Those pole-zero pairs do not all lie in the complex plane segments appropriate for the simplest Lipperheide-Fiedeldey process, and in fact we used their mixed rational-nonrational approach [12] to specify the quantal inversion potential.

B. The semiclassical (WKB) method

The semiclassical WKB method [13] is centered upon a quasipotential which can be written as

$$Q(\sigma) = \frac{4E}{\pi}\frac{1}{\sigma}\frac{d}{d\sigma}\left(\int_\sigma^\infty \frac{\delta(\lambda)}{\sqrt{\lambda^2-\sigma^2}}\lambda d\lambda\right) , \tag{16}$$

where λ is the angular momentum variable and $\delta(\lambda)$ is the phase shift function. That latter function relates to the S function by

$$S(\lambda) = e^{2i\delta(\lambda)} , \tag{17}$$

and the cross sections are defined by the values of those S functions with $\lambda = l+\frac{1}{2}$. The scattering potential can be determined uniquely from the Sabatier transformation,

$$V_{\rm WKB}(r) = E\left[1-e^{\left(\frac{-Q(\sigma)}{E}\right)}\right] , \tag{18}$$

provided that there is a one to one correspondence between r and σ, given by the transcendental equation

TABLE II. The poles of $S_{\rm rat}$ used in both the quantal and (exponential) WKB inversion calculations.

	α_1	α_2	α_3
Re	28.9597248	28.8606003	21.8403179
Im	−13.1957820	6.56645583	10.8426396

$$r = \frac{\sigma}{k} e^{\left(\frac{Q(\sigma)}{2E}\right)}. \tag{19}$$

Thus one needs to solve the integration over phase shift functions and Vollmer [14] has listed a number of different phase functions of pertinence to such a semiclassical analysis of atom-atom scattering for which that integration is analytic. Of that list, we have used the phase function of the form

$$\delta_0(\lambda) = -b_0 \lambda K_1(b_1 \lambda) \ , \tag{20}$$

which involves a modified Bessel function, as the quasipotential corresponding to $\delta_0(\lambda)$ is

$$Q_0(\sigma) = b_0 e^{-b_1 \sigma}. \tag{21}$$

For positive b_0, this "reference" quasipotential corresponds to a rapidly decreasing potential $V(r)$.

Another useful form of an S function (or phase shift function) is that considered by Lipperheide and Fiedeldey [15]. They have shown that an S function of the rational form, Eq. (11), gives a quasipotential

$$Q_R(\sigma) = 2iE \sum_m \left[\frac{1}{\sqrt{(\sigma^2 - \alpha_m^2)}} - \frac{1}{\sqrt{(\sigma^2 - \beta_m^2)}} \right]. \tag{22}$$

This form of S function, often used in conjunction with a reference S function as per Eq. (15), has been used with some success in WKB inversion of nuclear [8], electron-atom [10], and electron-molecule [11] scattering data.

In this study of atom-atom scattering we have considered an S function of the product form. In our first study we used the modified Bessel function form (of phase shifts) to specify the reference S function, and thereby the reference quasipotential. But we have also used as the reference the quasipotential that we found numerically from the phase shifts determined by the exponential coordinate space potential used in the fully quantal study. With the first case, to ensure that the WKB analysis is based upon the starting S matrix values that were used in the quantal inversion study, it was necessary to search for a new set of rational pole-zero pair values for the rational function part of the product. With the latter, the quantal inversion pole-zero pair values were used explicitly and so the S functions have the same values at all real integer angular momenta values. Consequently, the associated inversion potential is the appropriate one to match to the fully quantal inverse result.

Thus we have two WKB studies, with quite different reference S function forms, but which overall are in very good agreement between themselves and with the quantal inversion S function at the physical values of angular momenta. With the modified Bessel function case, when values of b_0 and b_1 of 0.18 and 3.996, respectively, define the background phase shift function, the set of ten complex conjugate pole-pair parameters, $\{\alpha_i, \beta_i\}$, listed in Table III gave us the desired extremely close fit to the quantal S function at the physical l values.

TABLE III. The poles of $S_{\rm rat}$ for the WKB inversion.

	Re	Im
α_1	34.25597730	−16.6388907
α_2	22.87918684	−6.48949172
α_3	17.84158077	−5.38368412
α_4	13.34528341	−5.17797907
α_5	0.2357497977	−0.56856095
α_6	3.178899896	2.511798649
α_7	5.801666798	3.539298069
α_8	29.18965504	7.073164948
α_9	12.80543753	15.06738949
α_{10}	33.13973690	15.09356482

IV. RESULTS AND DISCUSSION

The cross sections from the elastic scattering of 62.5 meV He atoms from Ne atoms are shown in Fig. 1. In the inset, the measured data [4] are displayed by the dots with error bars and they are compared with the result of our deconvolution calculation (solid curve). The values of that deconvoluted cross section at the stipulated experimental scattering angles then are displayed by the dots in the main body of this figure (the error bars are the empirical ones again) and are what will be referred to hereafter as the data. All χ^2/F values are defined with respect to the fit of a calculated cross section to that set of (deconvoluted) data. The cross sections with which this data are compared were obtained by using the quantal inversion, a (modified) WKB inversion, and a Hartree-Fock

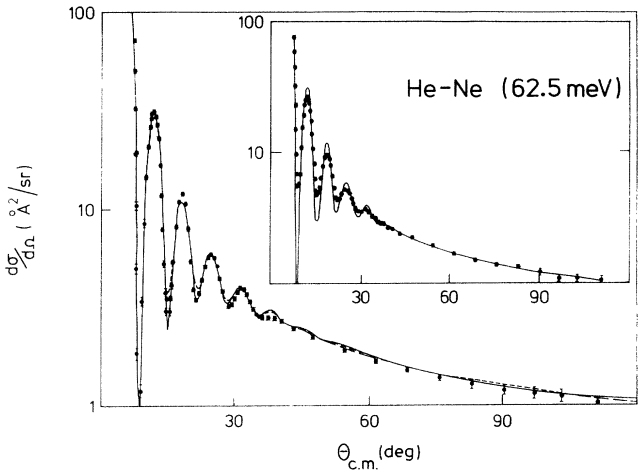

FIG. 1. The differential cross sections for elastic scattering of 62.5-meV He atoms from Ne atoms. The "data" obtained from deconvolution are displayed in the larger segment by the dots. The solid line shown therein was obtained from the quantal inversion. The short dashed line displays the WKB inversion result while the long dashed line represents the cross section found by using a potential from a Hartree-Fock calculation. The inset shows the effect of deconvoluting the diffraction oscillations of the actual measured data (dots).

calculated [7] potential, respectively, to give the solid, short dashed, and long dashed curves. Clearly the results are all very similar and graphically (this scale) they seem to be very good fits to the data. For this reason only the inversion cross section obtained by using the exponential form for a potential to specify the background quasipotential has been shown. The result is designated as modified since a short range potential had to be added to the WKB one. WKB potentials are defined only to the turning point (≈ 2.1 Å). To use them in finding solutions of the radial Schrödinger equations then requires a continuation to smaller radii. We used the values of the quantal inversion potential at those small radii.

With the inversion potentials, the fits to the data are epitomized by values of χ^2/F of 14.7 and 18.8, respectively. The Hartree-Fock result gave a value of 29.9. All three results are too large for us to make a confidence level assessment of the radial values of these potentials as was possible in studies of electron scattering using inverse scattering theory [10], and we note that 90% of the χ^2 value comes from the angular region between 6.5° and 26.5°.

Four (real) potentials are shown in Fig. 2 with the solid, dotted, short dashed, and long dashed curves portraying the quantal inversion, the (exponential) WKB, inversion, the (Bessel background) WKB, and Hartree-Fock interactions, respectively. Clearly, the quantal inversion potential has a deeper minimum value than the others with the two WKB results lying between that and the theoretically calculated one. All three inversion potentials decrease more slowly at large radii than does the Hartree-Fock interaction, and all three inversion potentials are indistinguishable on this scale from 4 Å outwards.

It is known [15] that potentials associated with the class of rational S functions we have used in the inversion calculations asymptote as $\frac{1}{r^3}$. That is not the $\frac{1}{r^6}$ character one may expect for interatomic interactions. But the asymptotic value is a good approximant only at very large radii. In any event, the data are not very sensitive to the exact long range nature of this interaction (i.e., beyond ≈ 4 Å). To ascertain that, we solved the radial Schrödinger equations using the quantal inversion potential up to a cut off radius R_{cut}, and matched on a $\frac{1}{r^6}$ tail at larger radii. From those calculations χ^2/F values of 47.2, 16.5, 16.2, and 16.0 were obtained from the fit to data when cutoff radii of 3.0, 3.5, 4.0, and 6.0 Å were used. Those numbers are to be compared with a value of 14.7 from use of the undoctored potential. The value of 3.0 Å for R_{cut} is practically at the potential well minimum. There is a similar insensitivity to the exact behavior of the potentials at small radii too. By varying the quantal inversion potential to be a constant within a lower radius R_{low}, calculated cross sections gave χ^2/F values of 79.2, 16.1, and 15.8 when R_{low} was set at 2.16, 2.15, and 2.0 Å, respectively.

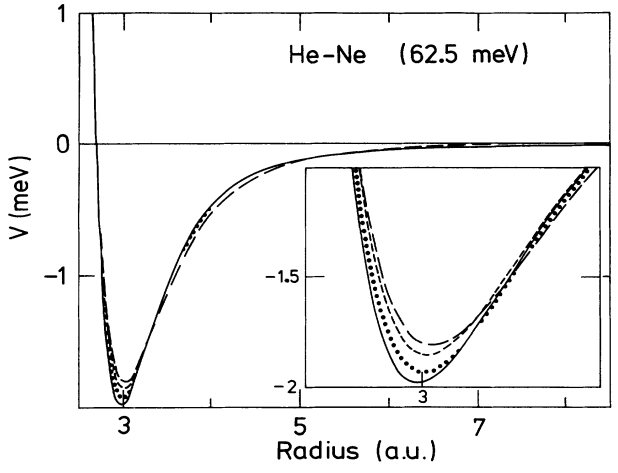

FIG. 2. A comparison of the diverse He-Ne interatomic potentials. The solid, short dashed, dotted, and long dashed lines represent the potentials obtained from the quantal inversion, the Bessel background (WKB) inversion, the (exponential) WKB inversion, and the Hartree-Fock calculations, respectively.

To investigate the semiclassical (WKB) method, not only have we used the same product S function defined for the quantal approach, but also we mapped that S function to the Bessel reference form to have equivalent phase shifts from l=0 to l=200. The quality of that match is reflected by a total χ^2, defined as $\chi^2 = \sum_{l=0}^{200} |S_{\text{WKB}} - S_{\text{quantal}}|^2$, less than 0.7×10^{-4}. From Fig. 2 we note that the quantal and both WKB inversion potentials coincide very well except at around 3 Å where the potentials have a minimum. With the (exponential) WKB potential, its variation from the quantal result reflects the effect of the WKB approximation. But there are also differences between the two WKB potentials. The two S_{WKB} have different functional forms, so that the interpolation and/or extrapolation they make upon the set of (physical) phase shifts has led to these quite different potentials. To verify these conjectures, it is necessary to check that use of the WKB inversion potentials in direct solution of the Schrödinger equations reproduces the input S function. However, the WKB inversion potential is not specified at radii less than the classical turning point. But at $r = 2.2$ Å, the WKB inversion potential has not reached the classical turning point and it is equal in value there to the quantal inversion potential; the reason for our choice of matching at low radii before. To study the sensitivity of the resultant phase shifts to the exact short range nature of the interaction, we made calculations varying both quantal and WKB inversion potentials by setting $V(r) = V(2.2\text{ Å}) = 48.19$ meV for $r < 2.2$ Å. The phase shifts that result are compared with those of other interaction forms in Fig. 3.

The solid curve in Fig. 3 displays the phase shifts we obtained by using the full quantal inversion potential. The full WKB phase shift values are indistinguishable from that on this scale. But when the short ranged potentials are set to a constant, the results do differ noticeably from the complete ones. The cutoff cases are displayed by the long dashed curve in Fig. 3. Also shown in this figure are the phase shifts associated with diverse component S functions. The short dashed curve displays the phase shifts of the exponential background potential

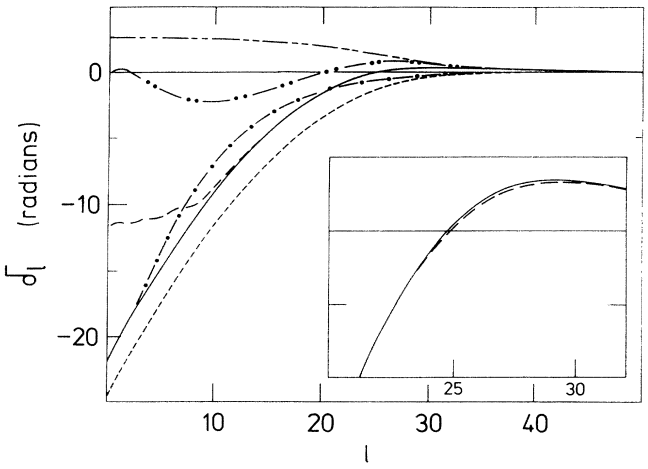

FIG. 3. Recalculated He-Ne scattering phase shifts as functions of the angular momentum l and compared with the empirical function (solid curve). The results of calculations displayed by the other curves are defined in the text. The inset shows the important l value phase shifts of the fitted (solid curve) phase shifts in comparison with those found by solving the Schrödinger equation directly with the WKB potential (dashed curve). The quantal result is indistinguishable from the fitted values on this scale.

and those of the (quantal) rational part are shown by the long-short-short dashed line. The Bessel function S function gives the phase shift variation displayed by the dash-dot-dot curve and the rational function associated with that led to the result shown by the dash-dot curve.

In the inset in Fig. 3, the full quantal and both WKB results for $l > 22$ are compared. The differences are small although the (Bessel) WKB phase shifts in that range are smaller positive values; a consequence of the smaller attractive part of the associated potential. To the extent shown, WKB inversion does not reproduce the starting phase shifts. The discrepancy between the (exponential) WKB and the quantal inversion thus is due to the inaccuracy of the WKB approximation at this energy. That also reflects in the cross section fits as the WKB calculation gave a χ^2/F of 18.8; a value that is $\approx 30\%$ larger than that obtained by the quantal inversion analysis.

V. CONCLUSIONS

Some He-Ne potentials in the literature are summarized in Ref. [4]. All the potentials have well depths of 1.8–2.0 meV, minimum points, and zero crossings within 0.03 Å of 3.00 Å and 2.68 Å, respectively. Of all potentials compared, ours found by inversion included the best fit to the deconvoluted data; namely, that found by quantal inversion. But no case gave fitting values of χ^2/F near to the statistically significant value of 1. As a consequence we are as yet unable to place confidence levels upon the radial values of the inversion potentials. Clearly they reflect the expected shape, however. But there is quite a variation in the specific values of these atom-atom potentials in the region of (weak) attraction. The quantal inversion result is favored, however, as the procedure is more accurate than the WKB scheme and, notably, gives the potentials inside of the classical turning point.

ACKNOWLEDGMENTS

The financial support of a DITARD grant to assist with these studies, and under the Australian–Peoples Republic of China scientific exchange program, is gratefully acknowledged.

[1] R. S. Mulliken and W. C. Ermler, *Diatomic Molecules* (Academic, New York, 1977); H. Margenau and N. R. Kestner, *Theory of Intermolecular Forces* (Pergamon, New York, 1971).
[2] J. P. Toennies, in *Physcial Chemistry, an Advanced Treatise*, edited by D. Hinderson (Academic, New York, 1973), Vol. IV, Chap. 6.
[3] *State-selected and State-to-state Ion-Molecule Reaction Dynamics*, edited by M. Baer and C. Y. Ng (Wiley, New York, 1992), Vols. I, II.
[4] M. Keil, L. J. Danielson, U. Buck, J. Schleusener, F. Huisken, and T. W. Dingle, J. Chem. Phys. **89**, 2866 (1988).
[5] K. Chadan and P. S. Sabatier, *Inverse Problems in Quantum Scattering Theory*, 2nd ed. (Springer, Berlin, 1989).
[6] U. Buck, Comput. Phys. Rep. **5**, 1 (1986).
[7] M. Shapiro and R. B. Gerber, J. Chem. Phys. **67**, 3570 (1977).
[8] L. J. Allen, K. Amos, C. Steward, and H. Fiedeldey, **41**, 2021 (1990); L. J. Allen, H. Fiedeldey, S. A. Sofianos, K. Amos, and C. Steward, *ibid.* **44**, 1606 (1991); L. J. Allen, K. Amos, and H. Fiedeldey, J. Phys. G **18**, L179 (1992).
[9] L. J. Allen, L. Berge, C. Steward, K. Amos, H. Fiedeldey, H. Leeb, R. Lipperheide, and P. Fröbrich, Phys. Lett. B **298**, 36 (1992).
[10] L. J. Allen, Phys. Rev. A **34**, 2708 (1986); L. J. Allen and I. E. McCarthy, *ibid.* **36**, 2570 (1987).
[11] A. Lun, L. J. Allen, and K. Amos, Phys. Rev. A **49**, 3788 (1994).
[12] H. Leeb, W. A. Schnizer, H. Fiedeldey, S. A. Sofianos, and R. Lipperheide, Inverse Problems **5**, 817 (1989).
[13] H. Fiedeldey, R. Lipperheide, K. Naidoo, and S. A. Sofianos, Phys. Rev. C **30**, 434 (1984).
[14] G. Vollmer, Z. Phys. **226**, 423 (1969).
[15] R. Lipperheide and H. Fiedeldey, Z. Phys. A **286**, 45 (1978); **301**, 81 (1981).